

Enhancement of the Dissolution of Nutrient Elements from Steelmaking Slag into Seawater by Gluconic Acid

Xiaorui Zhang · Hiroyuki Matsuura ·
Fumitaka Tsukihashi

Published online: 21 March 2015
© The Minerals, Metals & Materials Society (TMS) 2015

Abstract Steelmaking slag has been buried in coast to provide nutrient elements, especially iron, into seawater for the seaweeds' growth. However, the solubility of iron is extremely low under the oxic seawater conditions. In order to stabilize soluble iron which is dissolved from steelmaking slag into seawater, the addition of gluconic acid was investigated in the present study. By using two kinds of synthesized steelmaking slag with different CaO/SiO₂ ratios, the effect of gluconic acid on the dissolution behavior of various elements into seawater, while varying the concentration of gluconic acid and pH, was studied. The dissolution of Ca, Si, P, and Fe was greatly enhanced by the addition of gluconic acid and their concentration increased for increasing gluconic acid concentration. The dissolution mechanisms of each element were discussed using their stability diagrams and the dissolution reactions.

Keywords Recycling · Steelmaking slag · Coastal environment · Gluconic acid · Seawater · Dissolution behavior

Introduction

Utilization of steelmaking slag is indispensable for sustainable growth of the steelmaking industry. Steelmaking companies are now seeking new technologies to reduce the amount of steelmaking slag and meet the demand of transforming the slag into a valuable resource. It has been reported by Nakamura et al. [1] that phytoplankton grows positively in cultures with the addition of steelmaking slag, which indicates that steelmaking slag is an effective solution to sea desertification. The latter is also called ISOYAKE or barren grounds along the coastal areas and has been identified as a serious environmental problem not only in Japan but also all over the world. Many measures are used for recovering the now extinct seaweed beds: one of the feasible long-term candidates is steelmaking slag because of its reasonable cost, sufficient quantity, adequate mineral concentration, and the nature of its ionic structure [2, 3].

Among the bioactive trace metals, iron is an essential micronutrient element for the multiplication of phytoplankton [1]. Futatsuka et al. [2, 4], Arita et al. [5], and Sugie and Taniguchi [6, 7] have confirmed that nutrient elements such as Fe, Si, and P can dissolve from steelmaking slag into seawater. However, in oxic seawater, the solubility of iron is extremely low at the normal pH range of seawater [5–9]. Hence, it is necessary to adopt an efficient way to stabilize soluble Fe in seawater.

Hydroxycarboxylic acids such as sugar acids are generally released from phytoplankton. As one kind of sugar acid, gluconic acid (HG_{H4}) is biologically quite important in living organisms [8]. High concentration of gluconic acid (0.7–0.8 μM) was detected in surface seawater during spring bloom in Funaka Bay (Japan) coincident with the elevated dissolved Fe(II) [8, 10, 11]. Therefore, it is of great value to investigate the enhancement effect of

X. Zhang · H. Matsuura (✉) · F. Tsukihashi
Department of Advanced Materials Science, Graduate School of
Frontier Sciences, The University of Tokyo, 5-1-5-501
Kashiwanoha, Kashiwa, Chiba 277-8561, Japan
e-mail: matsuura@k.u-tokyo.ac.jp

F. Tsukihashi
e-mail: tukihashi@k.u-tokyo.ac.jp

Present Address:

X. Zhang
Graduate School of Pure and Applied Sciences, University of
Tsukuba, 1-1-1 Tennodai, Tsukuba, Ibaraki 305-8573, Japan
e-mail: xr_zhang@ims.tsukuba.ac.jp

gluconic acid on the dissolution of the elements from steelmaking slag into seawater.

In the present study, the dissolution behavior of Ca, Si, P, and Fe from steelmaking slag into seawater was investigated in laboratory-scale experiments, while varying the concentration of gluconic acid and pH. The dissolution mechanisms of the elements were also clarified by using the solubility diagrams in seawater and the potential–pH diagram of iron–water system. Moreover, the mineralogical phases of steelmaking slags before and after shaking experiments were investigated by X-ray diffraction (XRD).

Experimental

Materials

Two kinds of slags were examined in the present study and are identical to those used in the previous work [3]; the particle size was under 150 μm. The slags were prepared by melting a mixture of produced CaO and FeO, and reagent grade SiO₂ and Ca₃(PO₄)₂·xH₂O, at 1723 K for 50 min, under Ar flow of 1 L/min, and quenching on a steel plate by jetting Ar gas. Their compositions are shown in Table 1. Under the synthesis conditions, slag S-1 was completely melted, as predicted in the CaO–SiO₂–FeO_x ternary phase diagram [12], while slag S-2 was partly melted because of its high liquidus temperature.

The phases of slags S-1 and S-2 were characterized by powder X-ray diffraction (XRD: M18XHF, Mac Science,

Japan) with a Cu-Kα radiation source (λ = 1.5406 Å) at 40 kV and 200 mA over a range between 20° and 80°. Figure 1 shows XRD patterns of the synthesized slags S-1 and S-2. XRD patterns revealed that slag S-1 was composed of CaO·FeO·SiO₂ phase, and slag S-2 was composed of 2CaO·SiO₂ phase and FeO phase. The phases detected by XRD analysis were consistent with those predicted by the CaO–SiO₂–FeO_x ternary system.

Artificial seawater was made by dissolving a specific amount of artificial seawater raw materials (“Aquamarine” supplied by BizScience company, Japan) into 20 L distilled water and adjusting pH to around 8.2 by adding 0.13 mol/L NaOH solution. Its composition is shown in Table 2.

The 0.12, 0.25, or 0.50 g/L gluconic acid–seawater solution was prepared in advance before each experiment. First, the pH of 50 % gluconic acid (analytic reagent grade, Wako Pure Chemical Industries, Ltd., from 47.0 to 53.0 mass %, density: 1.24 g/cm³) was adjusted to 8.3 by NaOH solution, and then this gluconic acid was diluted 100 times by seawater to prepare the solution with 6.2 g/L and pH of 7.74. Subsequently, 0.12, 0.25, or 0.50 g/L gluconic acid–seawater solution was synthesized and their final pH values were 7.60, 7.47, and 7.45, respectively.

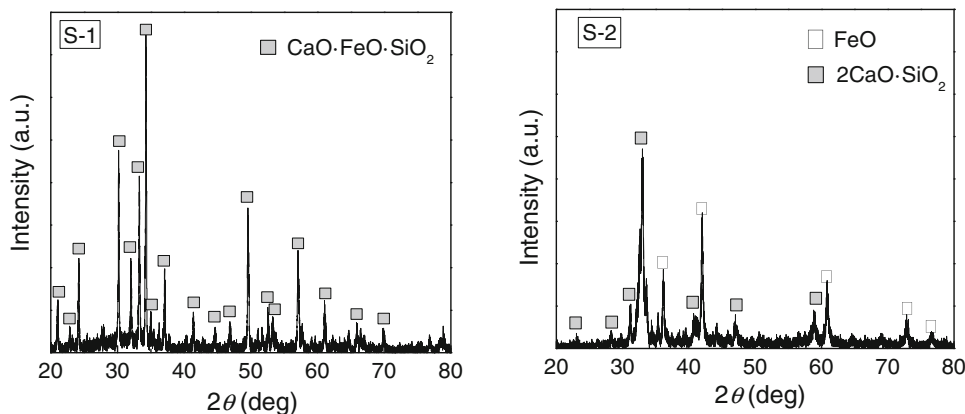
Shaking Procedure

The shaking experiments were conducted in batches, in the same manner as that of the previous study [3]. The oscillation speed was 160 cycles/min with an amplitude of 20 ± 5 mm, and the shaking time varied from 1 to 96 h (4 days). One gram of slag was added into 100 mL of artificial seawater–gluconic acid solution in a 250 mL of polyethylene bottle. The shaking experiments of 1 g slag/100 mL seawater or 100 mL of seawater without slag were also conducted for comparison. After shaking, the pH and oxidation–reduction potential (ORP) of the shaking solution were measured immediately by a pH meter (IM-55G

Table 1 Compositions of synthesized slags (mass %)

slag	FeO	CaO	SiO ₂	P ₂ O ₅	CaO/SiO ₂
S-1	30.0	33.8	33.7	2.5	1.0
S-2	30.0	45.0	22.5	2.5	2.0

Fig. 1 XRD patterns of synthesized slags S-1 and S-2



with GST 5731C probe, DKK-TOA Corp.) and an ORP meter (HM-25R with PS-5111C probe, DKK-TOA Corp.). The reference electrode of the ORP probe is Ag/AgCl, and thus ORP values shown below are those after conversion against the standard hydrogen electrode. Subsequently, the solution was filtrated with a 0.45 μm Millipore membrane filter. The concentrations of Ca, Mg, and Si were measured by an inductively coupled plasma optical emission spectrometer (ICP-OES, Seiko Instruments Inc., SPS7800 Plasma Spectrometer), and the concentrations of Fe and P were examined by the modified molybdenum blue spectrometric method and the modified 1,10-phenanthroline spectrometric method, respectively. Furthermore, the phases of the slags after shaking experiments were also examined by XRD.

Results and Discussion

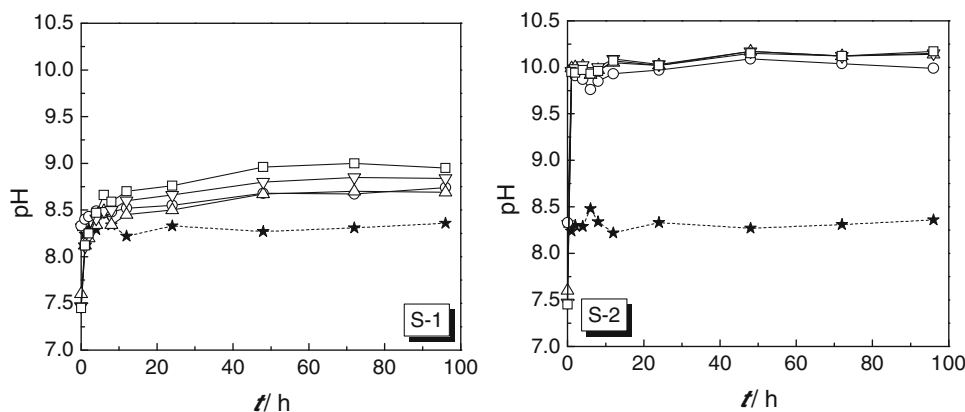
Variation of pH

Figure 2 shows the variation of pH with time for seawater containing various concentrations of gluconic acid. For

Table 2 Chemical composition of artificial seawater

Constituent	Concentration (mg/L)
NaCl	24,534
MgCl ₂ ·6H ₂ O	11,112
Na ₂ SO ₄	4094
CaCl ₂ ·2H ₂ O	1535
KCl	695
NaHCO ₃	201
KBr	101
SrCl ₂ ·6H ₂ O	43
H ₃ BO ₃	27
NaF	3

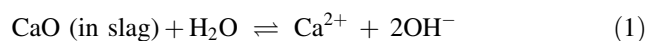
Fig. 2 Variation of pH with time for seawater containing various concentrations of gluconic acid. Gluconic acid (g/L): —○— 0, —△— 0.12, —▽— 0.25, —□— 0.50, —★— Seawater



both slags, pH increased dramatically in the beginning; however, for prolonged shaking time, the pH increase was only moderate for slag S-1 and stable around 10.1 for slag S-2. As illustrated in our previous work [13], the buffering action provided by the dissociation of gluconic acid is negligible. In the case of slag S-1, pH increased with increase of concentration of gluconic acid. The highest pH value was approximately 9.0 with 0.4 g/L gluconic acid. In the case of slag S-2, the variation of pH with the gluconic acid concentration was not obvious, whereas pH was slightly higher than that without addition of gluconic acid. The pH of solution with slag S-2 was much higher than that of slag S-1, which is the same as that in the previous work [13].

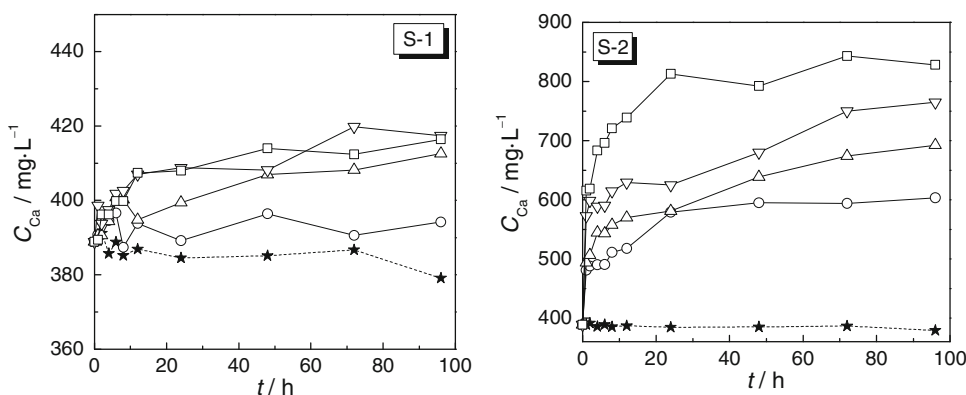
Dissolution of Ca and Concentration Change of Mg

Figure 3 shows the dissolution behavior of Ca from slags S-1 and S-2 into seawater with various concentrations of gluconic acid. The concentration of Ca increased upon increasing both the shaking time and the concentration of gluconic acid, while it was much higher in the case of slag S-2 than that of slag S-1. After 96 h shaking, the concentration of Ca changed from 394 to 417 mg/L for slag S-1 and from 604 to 828 mg/L for slag S-2. For slag S-1, the concentration of Ca in seawater with gluconic acid was larger than that without gluconic acid, while for those solutions with 0.25 and 0.50 g/L gluconic acid were similar. Since the dissolved amount of Ca from slag S-1 was small, the dissolution behavior of Ca was largely influenced by other elements contained in seawater. In the case of slag S-2, the increment of Ca concentration was followed by the concentration of gluconic acid. The dissolution of Ca from slag into seawater is expressed by reaction (1) [14–16].

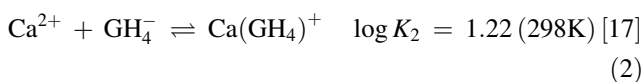


Dissolution of CaO is enhanced by the complexation reaction between Ca and gluconic acid such as reaction (2)

Fig. 3 Dissolution behaviors of Ca from slags S-1 and S-2 into seawater with various concentrations of gluconic acid. Gluconic acid (g/L): —○— 0, —△— 0.12, —▽— 0.25, —□— 0.50, —★— Seawater



[17]. Hence, pH increased with increasing the concentration of gluconic acid for slag S-1.



where GH_4^- is the symbolic form of gluconate ion.

Despite the significant dissolution of Ca from slag S-2 on adding gluconic acid, pH was still constant around 10.1, which is attributed to the precipitation of Mg^{2+} contained in the original artificial seawater. Figure 4 shows the concentration change of Mg in seawater during shaking of slags S-1 and S-2, with seawater containing various concentrations of gluconic acid.

With slag S-1, the concentration of Mg changed in a small range between 1172 and 1217 mg/L, which is close to that of seawater. With slag S-2, the concentration of Mg decreased upon increasing both the shaking time and the concentration of gluconic acid. The smallest concentration of Mg was 918 mg/L after shaking for 96 h with 0.50 g/L gluconic acid.

Magnesium hydroxide has relatively lower solubility compared to calcium hydroxide and thus Mg^{2+} in the seawater precipitates as $\text{Mg}(\text{OH})_2$ by the substitution reaction (3) when pH reaches a certain value [3, 14–16]. Hence, the concentration change of Mg shows an opposite trend to that of Ca for slag S-2.

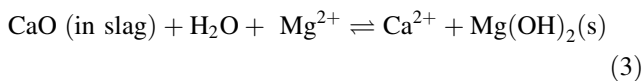
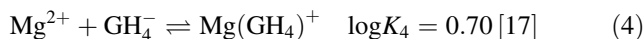


Figure 5 shows the relationship between the concentrations of Ca and Mg during shaking of slags S-1 and S-2. In the case of slag S-1, shown in Fig. 5a, the concentration of Mg was not affected by the increase in the concentration of Ca. In the case of slag S-2, shown in Fig. 5b, the concentration of Mg decreased linearly with increasing the concentration of Ca, regardless of gluconic acid concentration. However, the slopes of the linear regression lines are different for the solutions with and without gluconic acid,

which is due to the formation of magnesium–gluconate complex according to reaction (4) [17]. Since the soluble Mg concentration becomes higher, the slope of the linear regression line between Ca and Mg concentrations with gluconic acid is larger (less steep) compared to that without gluconic acid.



The concentrations of Ca and Mg are shown in the solubility diagrams of Ca and Mg in Fig. 6 [3]. The concentrations of Ca and Mg for slag S-1 are below the saturation line of $\text{Mg}(\text{OH})_2$. Therefore, pH increased slightly but the concentration of Mg did not change with the dissolution of Ca. The concentrations of Ca and Mg for slag S-2 are located above the saturation line of $\text{Mg}(\text{OH})_2$; hence, the concentration of Mg decreased, and pH was maintained at approximately 10.1 during the dissolution of Ca.

Dissolution of Si

The dissolution behavior of Si from slags into seawater containing gluconic acid is shown in Fig. 7. Depending on the CaO/SiO₂ ratio of slag, the dissolution behavior of Si was quite different. In the case of slag S-1 with the CaO/SiO₂ ratio of 1, the concentration of Si increased upon increasing both the shaking time and the concentration of gluconic acid. After 96 h shaking, the concentrations of Si were 5.13, 10.58, 15.80, and 20.13 mg/L in seawater with 0, 0.12, 0.25, and 0.50 g/L gluconic acid, respectively. The concentration of Si monotonically increased with increasing the concentration of gluconic acid. In the case of slag S-2 with the CaO/SiO₂ ratio of 2, the concentration of Si reached a maximum at the beginning of shaking, and then it decreased abruptly toward stable values. In general, the concentration of Si increased with increasing the concentration of gluconic acid. In the case of seawater, the soluble Si concentration varied from 0 to 2.09 mg/L. However, there is no Si element in the artificial seawater as shown in

Fig. 4 Concentration change of Mg in seawater during shaking of slags S-1 and S-2 with seawater containing various concentrations of gluconic acid. Gluconic acid (g/L): —○— 0, —△— 0.12, —▽— 0.25, —□— 0.50, —★— Seawater

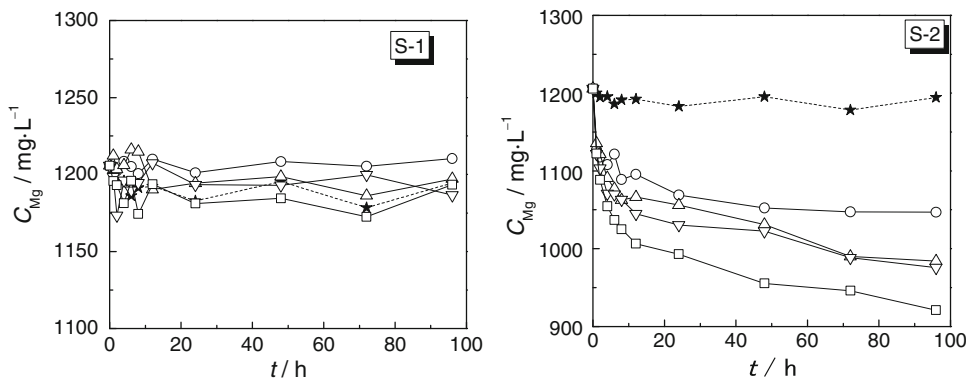


Fig. 5 Relationship between concentrations of Ca and Mg during shaking: **a** slag S-1; **b** slag S-2

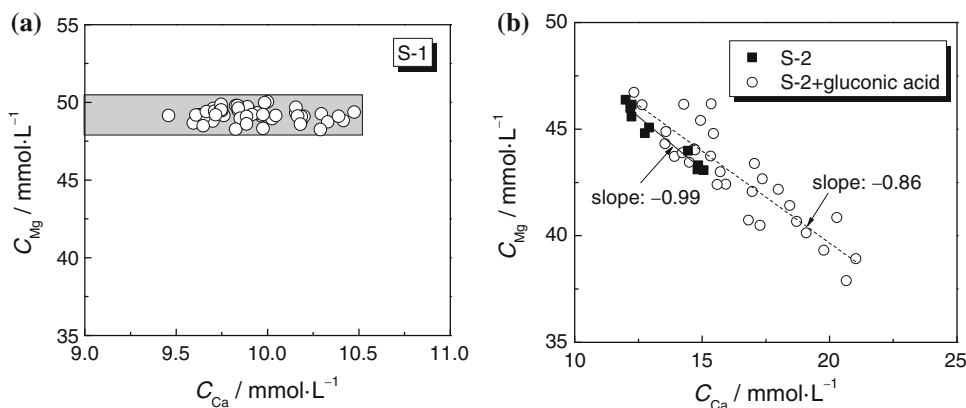
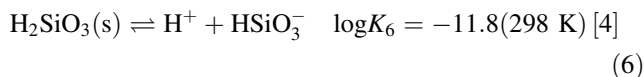
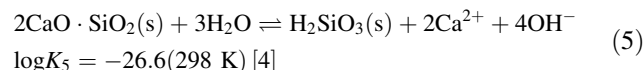


Table 2, and thus this result is attributed to an analytical error.

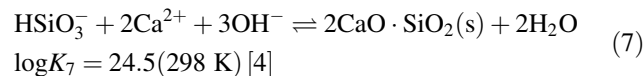
The solubility diagram of Si is used to clarify the dissolution mechanism of Si from steelmaking slag into seawater as shown in Fig. 8 [3]. Although the dissolution of Si from steelmaking slag into seawater was enhanced by

adding gluconic acid, it is still equilibrated with silicon hydrates as shown in the diagram.

For slag S-2, Si concentration is located in the region between H_2SiO_3 and H_4SiO_4 saturation lines, and its species is $HSiO_3^-$. Thus, the dissolution of Si from slag S-2 into seawater can be deduced by reactions (5) and (6) [3, 4, 18]:



With the fast dissolution of Ca from slag S-2 into seawater, according to reaction (5), solid H_2SiO_3 is formed. Then the concentration of Si increases as the reactions (5) and (6) proceed. On the other hand, Ca ion is supplied by the dissolution of some other phases. Subsequently, another reaction (7) becomes significant when the reactions (5) and (6) reach a certain extent.



When the reactions (5), (6), and (7) reach the steady state with the extension of the shaking time, the

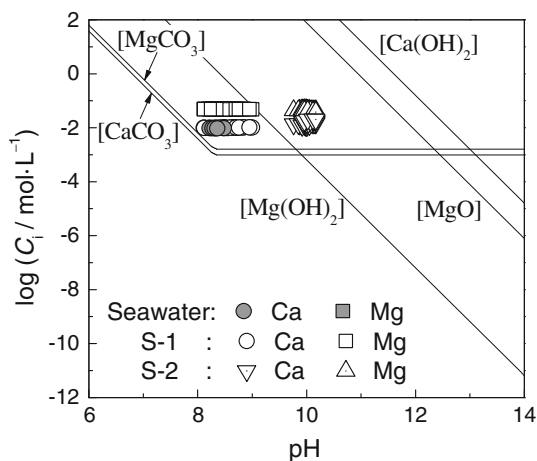


Fig. 6 Solubility diagram of Ca and Mg together with the shaking results

Fig. 7 Dissolution behaviors of Si from slags S-1 and S-2 with various concentrations of gluconic acid. Gluconic acid (g/L): —○— 0, —△— 0.12, —▽— 0.25, —□— 0.50, —★— Seawater

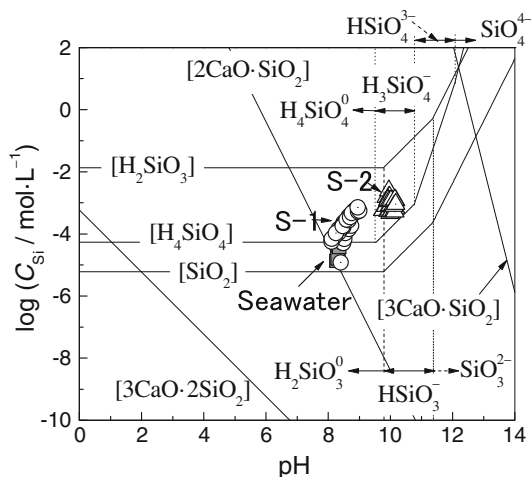
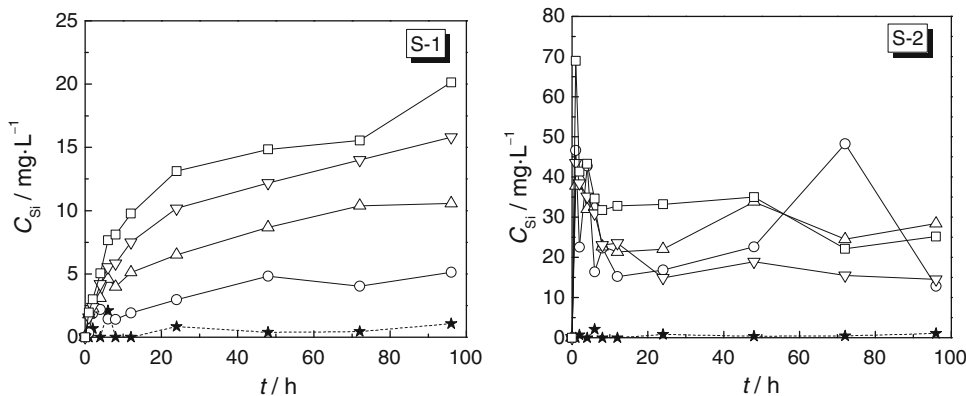


Fig. 8 Solubility diagram of Si together with the shaking results

concentration of Si becomes stable. Furthermore, due to the complexation reaction between Ca and gluconic acid, gluconic acid helps the reaction (5) proceed forward; hence, the concentration of Si increases with increasing the concentration of gluconic acid.

For slag S-1, the Si concentration is also located in the region between H_2SiO_3 and H_4SiO_4 phases, while Si mainly exists as $H_2SiO_3^0$. The dissolution of Si from slag S-1 into seawater is expected to be similar to that from slag S-2, which is the initial formation of silicon hydrate followed by the gradual dissolution into seawater. However, the reaction (7) is not taking place for slag S-1 because of the lower concentration of Ca, and thus, the concentration of Si monotonously increases with increasing shaking time.

Moreover, the enhancement of the dissolution of Si by gluconic acid can be attributed to the formation of silicon hydrate. Since gluconic acid is a weak polybasic acid, it is easier to give H^+ to the solid silica than water [reaction (5)] at the alkaline environment. Therefore, the larger concentration of gluconic acid is more favorable to form silicon hydrate which has larger solubility. Under the present

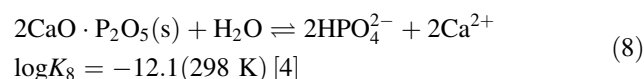
shaking conditions, the chelate between silicon and gluconic acid is expected not to form because both of them exist as anions.

Dissolution of P

The dissolution behavior of P from slags into seawater with various concentrations of gluconic acid is shown in Fig. 9. The dissolution behavior of P greatly depended on the CaO/SiO₂ ratio of slag. In the case of slag S-1, the concentration of P increased upon increasing both the shaking time and the concentration of gluconic acid. After 96 h shaking, the concentrations of P were 0.460, 1.358, 1.854, and 2.289 mg/L in seawater with 0, 0.12, 0.25, and 0.50 g/L gluconic acid, respectively. In the case of slag S-2, the soluble P was not detected in seawater without gluconic acid. The maximum concentration appeared in the beginning, and then P concentration decreased dramatically in the initial shaking period or even dropped below the detection limit. Comparing the dissolution behaviors of P from slags S-1 and S-2, the P concentration from slag S-2 is much lower than that from slag S-1, which reveals that slags with larger CaO/SiO₂ ratio effectively hinder the dissolution of P.

Figure 10 shows the solubility diagram of P together with the concentration of P dissolved from slags S-1 and S-2. The entire P concentration is located in the region between $2CaO \cdot P_2O_5$ and $Ca_3(PO_4)_2$ saturation lines, and the soluble species is HPO_4^{2-} . Thus, the dissolution of P can be expressed as reaction (8) [3].

For slag S-1, the chelation of the soluble Ca^{2+} is provided by gluconic acid, which makes reaction (8) proceed forward. Hence, the concentration of P becomes larger with larger concentration of gluconic acid.



For slag S-2, reaction (9) takes place simultaneously to control the concentration of P.

Fig. 9 Dissolution behaviors of P from slags S-1 and S-2 with various concentrations of gluconic acid. Gluconic acid (g/L): —○— 0, —△— 0.12, —▽— 0.25, —□— 0.50, —★— Seawater

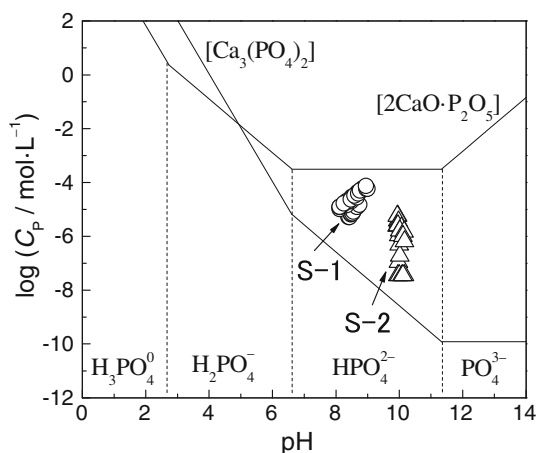
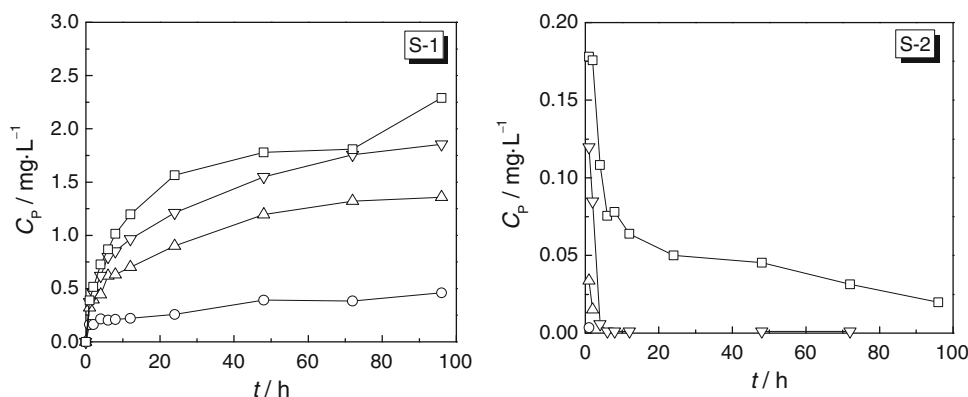
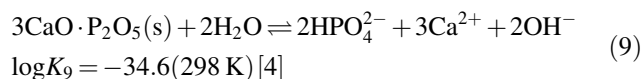


Fig. 10 Solubility diagram of P together with the shaking results



Reaction (9) proceeds backward when the concentration of Ca dissolved from slag S-2 increases dramatically (despite the chelation of soluble Ca^{2+} provided by gluconic acid), which subsequently results in the decrease of the P concentration in seawater. Therefore, the concentration of P decreases with increasing the shaking time.

Dissolution of Fe

The dissolution behavior of Fe from slags into seawater with various concentrations of gluconic acid is shown in Fig. 11. The soluble Fe was not detected in the seawater without gluconic acid for both slags S-1 and S-2. The CaO/SiO₂ ratio of slag determines the dissolution behaviors of Fe from slags into seawater. In the case of slag S-1, the dissolution of Fe increased with increasing the shaking time as well as concentration of gluconic acid. After 96 h

shaking, the concentrations of Fe were 12.12, 18.72, and 24.74 mg/L in seawater with 0.12, 0.25, and 0.50 g/L gluconic acid, respectively. In the case of slag S-2, the concentration of Fe decreased quickly before 12 h and then further decreased gradually with shaking time. After 96 h shaking, the concentrations of Fe were 0.01, 0.33, and 1.28 mg/L with 0.12, 0.25, and 0.50 g/L gluconic acid, respectively.

The variations of the ORP during the shaking of slags S-1 and S-2 with seawater containing various concentrations of gluconic acid are shown in Fig. 12. The ORP fluctuated in the initial shaking period and this phenomenon was smaller for shaking with slags compared to shaking of seawater. At the same time, the ORP in the case of shaking with slag S-2 was much smaller than that with slag S-1. Increasing the concentration of gluconic acid decreased the ORP.

The potential–pH diagram of iron–water system at 298.15 K with 10^{-6} mol/L soluble iron is shown in Fig. 13 [3] together with the measured ORP. The ORP of the shaking solution is located in the stable region of Fe₂O₃ phase, which implies that the concentration of soluble Fe is extremely low. However, the measured soluble Fe concentration in seawater with gluconic acid is much higher than that predicted by the potential–pH diagram of iron–water system.

Figure 14 [11] shows the solubility diagram of Fe with the shaking results. Soluble Fe during shaking of slag S-1 is in equilibrium with FeO and Fe(OH)₂ phases but larger than the equilibrium values. The soluble Fe species is considered to be Fe²⁺. On the contrary, the soluble Fe during shaking of slag S-2 is higher than the equilibrium value for Fe(OH)₃ and the soluble Fe species would be Fe(OH)₄⁻. This excess portion is attributed to the formation of iron–gluconate complexes.

For slag S-1, ferrous ion and gluconate ion form complex as reaction (10) suggests [20].

Fig. 11 Dissolution behaviors of Fe from slags S-1 and S-2 with various concentrations of gluconic acid

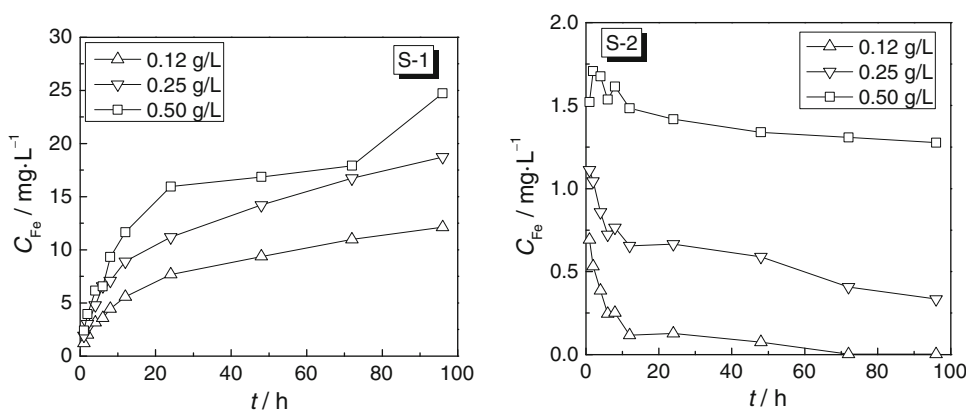


Fig. 12 Variation of ORP during the shaking of slags S-1 and S-2 with seawater containing various concentrations of gluconic acid. Gluconic acid (g/L): —○— 0, —△— 0.12, —▽— 0.25, —□— 0.50, —★— Seawater

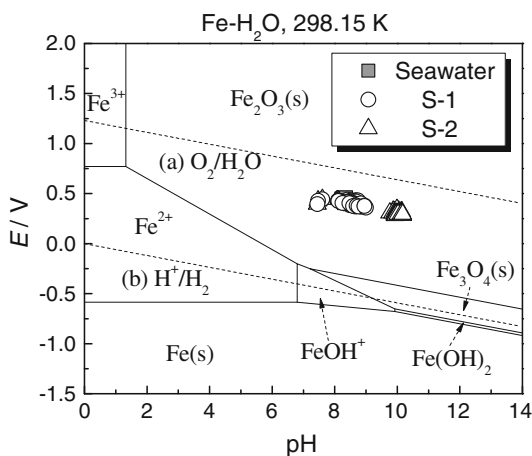
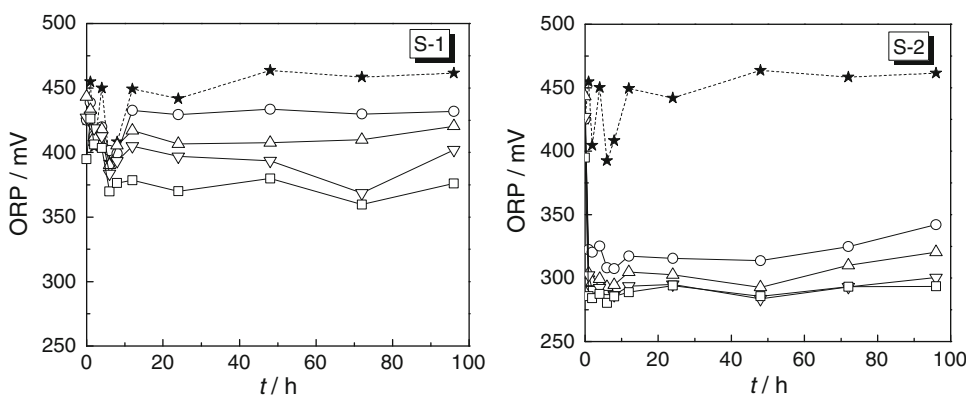


Fig. 13 Potential–pH diagram of iron–water system with the shaking results

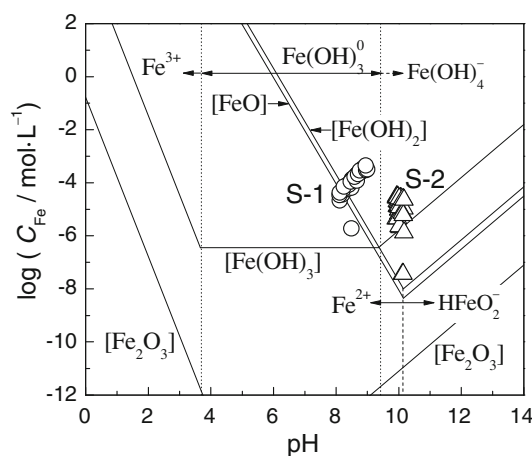
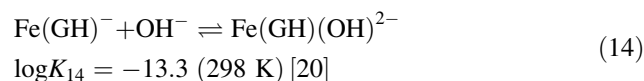
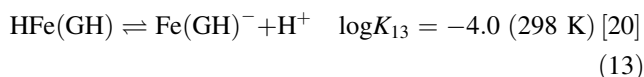
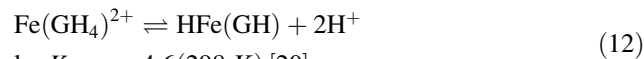
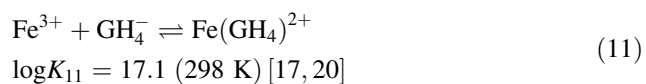


Fig. 14 Solubility diagram of Fe with the shaking results



For slag S-2, ferric ion and gluconate ion form a series of complexes with the increase of pH according to the following reactions (11–14) [17, 19–21]:



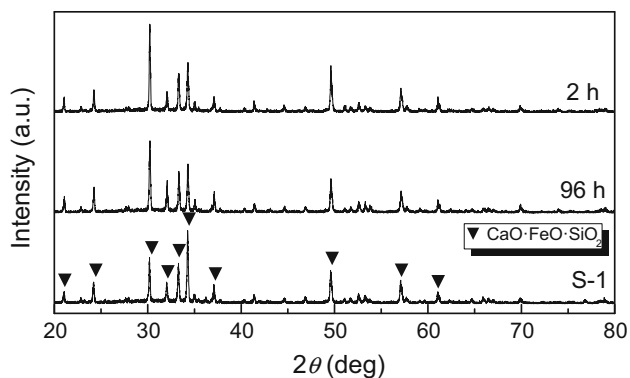


Fig. 15 XRD patterns of slag S-1 before and after shaking experiments

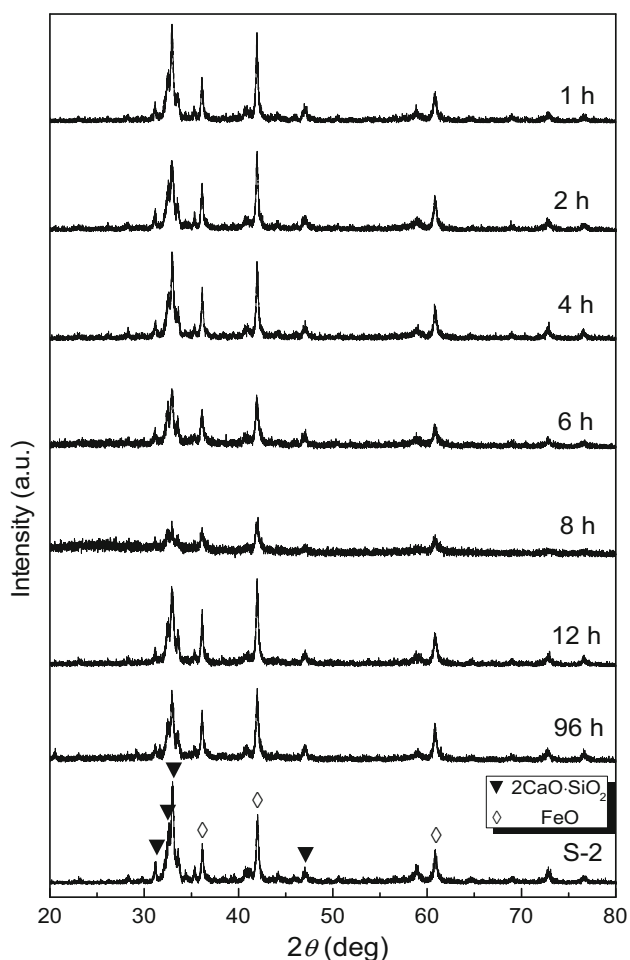


Fig. 16 XRD patterns of slag S-2 before and after shaking experiments

At higher pH regime, Fe^{3+} hardly exists, and it is prone to turn into $\text{Fe}(\text{GH})^-$ and $\text{Fe}(\text{GH})(\text{OH})^{2-}$ anions, and thus the concentration of Fe with slag S-2 is smaller than that

with slag S-1. On the other hand, the equilibrium constants of ferric-gluconate complexation reactions (11–14) decrease with increasing pH, which is another reason for the gradual decrease of soluble Fe with increase in shaking time. In addition, the ferric-gluconate complex is photoactive at large pH condition. Therefore, the gradual decrease in the concentration of Fe with time is due to the rapid photodegradation of the complex [22].

XRD Analysis of Steelmaking Slags

The XRD patterns of slags S-1 and S-2 before and after shaking experiments are shown in Figs. 15 and 16, respectively. The main peak positions in the diffraction patterns of the slags after shaking experiments are the same as those before shaking, which suggests that the main phases of slags do not change. Therefore, $\text{CaO}\cdot\text{FeO}\cdot\text{SiO}_2$ phase and $2\text{CaO}\cdot\text{SiO}_2$ and FeO phases mostly affect the dissolution behaviors of elements from slags S-1 and S-2, respectively.

Conclusions

The enhancement effect of gluconic acid on the dissolution of steelmaking slag into seawater was investigated by shaking experiments of slag and seawater with various shaking times and gluconic acid concentrations.

Because of the Ca-gluconate complex, pH for shaking slag S-1 increased upon increasing both the shaking time and the concentration of gluconic acid. On the contrary, pH for shaking slag S-2 was constant around 10.1 independent of the concentration of gluconic acid, which is due to the simultaneous buffering action of Mg^{2+} contained in the original seawater.

Dissolutions of Ca, Si, P, and Fe were enhanced by the addition of gluconic acid, but they largely depended on the CaO/SiO_2 ratio of slag. In the case of slag S-1 with the CaO/SiO_2 ratio of 1, the concentrations of Ca, Si, P, and Fe increased upon increasing both the shaking time and the concentration of gluconic acid. In the case of slag S-2 with the CaO/SiO_2 ratio of 2, the concentration of Ca increased upon increasing both the shaking time and the concentration of gluconic acid, while those of Si, P, and Fe decreased upon increasing the shaking time or decreasing the concentration of gluconic acid. The enhancement effect of gluconic acid on the dissolution of Si is due to the formation of silica hydrate having larger solubility; that on the dissolution of P is due to the masking action of Ca, which is beneficial to the existence of soluble P; and that on the dissolution of Fe is attributed to the formation of iron-gluconate complexes.

References

1. Nakamura Y, Taniguchi A, Okada S, Tokuda M (1998) Positive growth of phytoplankton under conditions enriched with steelmaking slag solution. *ISIJ Int* 38:390–398
2. Futatsuka T, Shitogiden K, Miki T, Nagasaka T, Hino M (2003) Dissolution behavior of elements in steelmaking slag into artificial seawater. *Tetsu-to-Hagané* 89(4):382–387
3. Zhang X, Matsuura H, Tsukihashi F (2012) Dissolution mechanism of various elements into seawater for recycling of steelmaking slag. *ISIJ Int* 52(5):928–933
4. Futatsuka T, Shitogiden K, Miki T, Nagasaka T, Hino M (2004) Dissolution behavior of nutrition elements from steelmaking slag into seawater. *ISIJ Int* 44:753–761
5. Arita K, Umiguchi Y, Taniguchi A (2003) Availability of steelmaking slag as a source of essential elements for phytoplankton. *Tetsu-to-Hagané* 89(4):415–421
6. Sugie K, Taniguchi A (2007) Bioavailability and dulability of the iron released from a steelmaking slag for tow *Thalassiosira* species. *Tetsu-to-Hagané* 93(8):558–564
7. Sugie K, Taniguchi A (2008) Continuation of bioavailability as an iron fertilizer of a steelmaking slag for two *Thalassiosira* species. *Tetsu-to-Hagané* 94(11):569–574
8. Kuma K, Nakabayashi S, Matsunaga K (1995) Photoreduction of Fe(III) by hydroxycarboxylic acids in seawater. *Water Res* 29(6):1559–1569
9. Baker AR, Croot PL (2010) Atmospheric and marine controls on aerosol iron solubility in seawater. *Mar Chem* 120(1–4):4–13
10. Nakabayashi S, Kudo I, Kuma K, Matsunaga K (1993) Trace determination of sugar acids (gluconic acid) in sea water by liquid chromatography. *Anal Chim Acta* 271(1):25–29
11. Kuma K, Nakabayashi S, Suzuki Y, Kudo I, Matsunaga K (1992) Photo-reduction of Fe(III) by dissolved organic substances and existence of Fe(II) in seawater during spring blooms. *Mar Chem* 37(1–2):15–27
12. Osborn EF, Arnulf M (1960) Revised and redrawn Phase equilibrium diagrams of oxide systems, Plate 7. American Ceramic Society and the Edward Orton, Jr., Ceramic Foundation
13. Zhang X, Atsumi H, Matsuura H, Tsukihashi F (2014) Influence of gluconic acid on dissolution of Si, P and Fe from steelmaking slag with different composition into seawater. *ISIJ Int* 54(6):1443–1449
14. Miki T, Shitogiden K, Samada Y, Nagasaka T, Hino M (2003) Consideration of dissolution behavior of elements in steelmaking slag based on their stability diagram in seawater. *Tetsu-to-Hagané* 89(4):388–392
15. Miki T, Futatsuka T, Shitogiden K, Nagasaka T, Hino M (2004) Dissolution behavior of environmentally regulated elements from steelmaking slag into seawater. *ISIJ Int* 44(4):762–769
16. Yamamoto T, Suzuki M, Oh SJ, Matsuda O (2003) Release of phosphorus and silicon from steelmaking slag and their effects on growth of natural phytoplankton assemblages. *Tetsu-to-Hagané* 89(4):482–488
17. Sawyer DT (1964) Metal-gluconate complexes. *Chem Rev* 64(6):633–643
18. Yokoyama S, Suzuki A, Izaki M, Umemoto M (2009) Elution behavior of electronic arc furnace oxidizing slag into fresh water. *Tetsu-to-Hagané* 95(5):434–443
19. Mehlretter CL, Alexander BH, Rist CE (1953) Sequestration by sugar acids. *Ind Eng Chem* 45(12):2782–2784
20. Pecsok RL, Sandera J (1955) The gluconate complexes. II. The ferric-gluconate system. *J Am Chem Soc* 77(6):1489–1494
21. Prescott FJ, Shaw JK, Bilello JP, Cragwall GO (1953) Gluconic acid and its derivatives. *Ind Eng Chem* 45(2):338–342
22. Rose AL, Waite TD (2002) Kinetic model for Fe(II) oxidation in seawater in the absence and presence of natural organic matter. *Environ Sci Technol* 36(3):433–444